NASA TT F-10,253

NASA TT F-10,253

PRODUCTION OF HIGH PLASMA VELOCITIES BY HEATING AND SELF-MAGNETIC ACCELERATION IN ELECTRIC ARCS

Th.Peters and K.Ragaller

Translation of "Erzeugung hoher Plasmageschwindigkeiten durch Heizung und eigenmagnetische Beschleunigung in Lichtbögen". Deutsche Versuchsanstalt für Luft- und Raumfahrt, Report No.372, October 1964, 41 pp.

NATIONAL AERONAUTICS AND SPACE ADMINISTRATION
WASHINGTON AUGUST 1966

German Aeronautics and Space Administration

Research Report 64-28

PRODUCTION OF HIGH PLASMA VELOCITIES BY HEATING AND SELF-MAGNETIC ACCELERATION IN ELECTRIC ARCS

Th.Peters and K.Ragaller

German Aeronautics and Space Experiment Station

October 1964

DVL Report 372 DK 533.95

PRODUCTION OF HIGH PLASMA VELOCITIES BY HEATING AND SELF-MAGNETIC ACCELERATION IN ELECTRIC ARCS*

Institute for Plasma Dynamics of the

German Aeronautics and Space Experiment Station

Stuttgart-Vaihingen, September 1964

Institute Director: Dr. Th.Peters

Authors: Dr. Th.Peters, K.Ragaller

* In cooperation with the Electrophysical Department of the Polytechnic Institute, Munich.
(Scientific Director: Prof. Dr. H.Maecker).

TABLE OF CONTENTS

NASA TT F-10,253

PRODUCTION OF HIGH PLASMA VELOCITIES BY HEATING AND SELF-MAGNETIC ACCELERATION IN ELECTRIC ARCS

*/4

Th.Peters and K.Ragaller

35958

Investigations are discussed on the increase in velocity of plasma jets by self-magnetic acceleration in electric arcs, using arc chambers in which the working gas is heated and then quasi-adiabatically expanded in an expansion nozzle. The arc operates not only inside the arc chamber at nearly constant pressure but also inside the expansion nozzle. Two modes of plasma acceleration are described: 1) heating of the plasma by the Joule heat produced in the arc; 2) magnetic acceleration produced by cooperation of current density and self-magnetic field (Lorentz forces). A device for realizing both effects, with the arc operating stably in an expanding supersonic flow at low and regular pressures, is described, with graphs showing the Lorentz forces in a plasma pinch, plasma jets with heating between cathode and anode, design of expansion nozzles of the cascade type, sketch of a device for rapidly expanding plasma flows, with plasma burner and auxiliary anode, etc. A comparison of magnetic acceleration for plasma engines with electrothermal engines, for various velocity ranges, is included.

author

* Numbers in the margin indicate pagination in the original foreign text.

Synopsis

35 958

Stationary plasma flows of high velocity had previously been produced with plasma burners, in which the working medium is heated in a combustion chamber by means of an electric arc and then is expanded in a nozzle in a quasi-adiabatic expansion.

The paper deals with the increase in velocity to be expected if the arc burns not only inside the arc chamber at nearly constant pressure but also in the expansion nozzle itself.

Two effects, contributing to plasma acceleration, are obtained:

1) During expansion, the plasma is reheated by the Joule heat, liberated in the arc, resulting in an increase in velocity.
2) In a divergent plasma flow with superposed arc, a magnetic acceleration effect is produced by cooperation of current density and self-magnetic field (Lorentz forces). This self-magnetic acceleration, at high current strength and low gas density, leads to extremely high velocities.

Decisive for a practical realization of both effects is the question whether an arc is able to operate stably in an expanding supersonic flow at low pressures. Experimental investigations demonstrate that this is the case.

author /7

1. Introduction

The dynamics of plasma furnishes data on the possibility of accelerating a plasma in the stationary state. Neglecting friction, radiation, and time-dependent terms, the fundamental equations will read as follows:

Continuity equation: $$div\, \rho \vec{v} = 0, \qquad (1.1)$$

Momentum equation: $$\varrho(\vec{v}\cdot\mathrm{grad})\vec{v} = -\mathrm{grad}\,p + \vec{j}\times\vec{B}\,, \tag{1.2}$$

Energy equation: $$\mathrm{div}\left[\left(\tfrac{1}{2}v^2+h\right)\varrho\vec{v} + \vec{W}\right] = \vec{j}\cdot\vec{E}\,. \tag{1.3}$$

In the stationary case, this is extended by the Maxwell equations

$$\mathrm{curl}\,\vec{B} = \mu_0\vec{j}\quad,\ (\mathrm{div}\,\vec{j} = 0) \tag{1.4}$$

and

$$\mathrm{div}\,\vec{B} = 0\,. \tag{1.5}$$

Compared to classical gas dynamics, two new terms occur in the conservation equations, namely, the Lorentz force $\vec{j} \times \vec{B}$ in the equation of momentum and the Joule heat $\vec{j} \cdot \vec{E}$ in the energy conservation equation. The law of conservation of energies stipulates that an electrically conducting gas can be heated or reheated by Joule heat $\vec{j} \cdot \vec{E}$.

Experimentally, this case is realized by using an electric arc. Specifically, in electrothermal plasma drives and plasma burners for wind tunnels, the gases are heated in arc chambers at high pressures and then - except for heat losses - adiabatically expanded in a nozzle. /8

The process itself is completely familiar in gas dynamics. The heating by combustion is replaced here by electric arc heating. The advantage lies in the fact that the obtainable temperatures and enthalpies in the arc chamber are no longer restricted by the reaction energies of the chemical partners but rather by the thermal stressability of the combustion-chamber walls which, at suitable cooling, can be pushed quite far upward. For numerous purposes, it is of advantage that gases of low molecular weight, such as hydrogen, helium, etc. can thus be heated. In any case, the maximum thermal stressability of the chamber walls and of the electrodes places an upper limit on the obtainable velocity which, for example in thermal plasma drives, is given as about 15,000 m/sec.

Another possibility of accelerating plasmas to high velocities is given by the occurrence of the Lorentz force $\vec{j} \times \vec{B}$ in the law of conservation of momentum. This force is predominantly utilized in short-time discharges, with which, within a time of 10^{-5} to 10^{-6} sec, plasma velocities of more than 10^5 m/sec can be obtained.

This electromagnetic acceleration process also includes the method of crossed fields, suitable for stationary operation. In this case, an already existing plasma is made to flow through a magnetic field, located perpendicular to the direction of flow, between two electrode plates. On applying a voltage, electric currents will start flowing across the plasma jet which, together with the suitably directed magnetic field, will generate forces in the direction of flow. It is known that this represents the inversion of an MHD generator and is based on the prototype of an electromagnetic direct-current pump for pumping of liquid metals. However, because of the high plasma temperature, considerable difficulties are produced by the rectangular geometry of the channel cross section, the boundary layer problem, and the electrode problem.

Below, we will investigate possibilities for combining the heating by /9
Joule heat $\vec{j} \cdot \vec{E}$ and the acceleration by Lorentz forces $\vec{j} \times \vec{B}$ in a stationary plasma flow in such a manner that optimum flow velocities are obtained.

Despite the fact that, in a plasma jet with arc heating, both effects are intimately connected, it is preferable to treat the effects separately. For this reason, we will first discuss the heating and, in a later Section, the effect of the Lorentz forces.

2. Flow with Arc Heating

The problem of heating a flowing gas not only in a heating chamber at relatively low velocities and high pressures but also in a subsequent expansion nozzle at high velocities, has been raised in numerous variants in propulsion projects.

Specifically, Ackeret and Winterberg (Bibl.1, 2) discussed this problem in connection with thermal nuclear rockets. In these, the upper limit of the exhaust velocity is defined by the maximum permissible temperature of the materials used in the reactor. However, theoretically, the possibility exists to modify the geometric structure of the reactor in such a manner that also the walls of the expansion nozzle will act as heat sources. Through this, the usual adiabatic expansion can be replaced, for example, by an isothermal expansion, which would lead to a higher exhaust velocity. Nevertheless, a more detailed study showed that the boundary layer problems, in the heat transfer from the nozzle wall to the gas, would lead to considerable difficulties.

It is logical to think of arc heating since, in this case, the heat is produced directly in the flowing plasma, provided that an arc is able to exist at all in an expanding supersonic flow. Similar to the material problems in nuclear rockets, the maximum obtainable combustion chamber temperature in a plasma drive, as mentioned above, is limited by the thermal stressability of the walls and electrodes, so that a reheating in the expanding flow seems promising.

A brief thermodynamic consideration will indicate the extent to which /10
the exhaust velocity can be increased. For simplicity, we will use an ideal gas with constant specific heat and one-dimensional flow as basis.

According to the law of conservation of energy, the heat supplied per unit mass is expressed by

$$dq = dh - \frac{1}{\rho} dp \,. \tag{2.1}$$

From the law of conservation of momentum, it then follows that

$$v\,dv = -\frac{1}{\rho}\,dp = dq - dh. \qquad (2.2)$$

In addition, the following equations are valid:

$$p = \rho\,\frac{kT}{m}, \qquad (2.3)$$

$$h = \frac{\varkappa}{\varkappa-1}\cdot\frac{p}{\rho} = \frac{\varkappa}{\varkappa-1}\cdot\frac{kT}{m}. \qquad (2.4)$$

Let us now compare the velocities, supplied amount of heat, and efficiencies in the case of polytropic and specifically isothermal and adiabatic expansion. Let us denote the combustion chamber factors by

$$p_0,\ \rho_0,\ T_0,\ h_0,\ (v_0 = 0),$$

while

$$p,\ \rho,\ T,\ h,\ v$$

are to denote the corresponding quantities after expansion.

<u>Velocities [Eq.(2.2)]</u> /11

<u>Polytropic</u>:

$$\frac{p}{\rho^n} = \frac{p_0}{\rho_0^n},$$

$$\frac{v^2}{2} = -\int_{p_0}^{p}\frac{dp}{\rho} = \frac{p_0^{1/n}}{\rho_0}\int_{p}^{p_0}\frac{dp}{p^{1/n}} = \frac{n}{n-1}\cdot\frac{p_0}{\rho_0}\left[1-\left(\frac{p}{p_0}\right)^{\frac{n-1}{n}}\right].$$

Taking eq.(2.4) into consideration, this yields

$$\frac{v^2}{2h_0} = \underset{(n>1)}{\frac{\varkappa-1}{\varkappa}\cdot\frac{n}{n-1}\left[1-\left(\frac{p}{p_0}\right)^{\frac{n-1}{n}}\right]} = \underset{(n<1)}{\frac{\varkappa-1}{\varkappa}\cdot\frac{n}{1-n}\left[\left(\frac{p}{p_0}\right)^{\frac{n-1}{n}}-1\right]}. \qquad (2.5)$$

<u>Isothermal (n = 1)</u>:

$$\frac{v^2}{2} = \frac{p_0}{\rho_0}\ln\frac{p_0}{p},$$

$$\frac{v^2}{2h_0} = \frac{\varkappa-1}{\varkappa}\ln\frac{p_0}{p}. \qquad (2.6)$$

<u>Adiabatic (n = x)</u>:

At n = x, eq.(2.5) gives

$$\frac{v^2}{2h_0} = 1 - \left(\frac{p}{p_0}\right)^{\frac{x-1}{x}} . \tag{2.7}$$

The ratio $\frac{v^2}{2h_0}$ is plotted in Fig.1 as a function of the pressure ratio p_0/p with $x = 5/3$ (monatomic gas) for various n. Whereas $\frac{v^2}{2h_0}$ tends toward 1 with increasing p_0/p in the adiabatic case, no limiting value exists in the isothermal case and at polytropic expansion at $n < 1$.

Supplied Quantities of Heat

In our model, a gas primarily receives an enthalpy h_0 in the combustion chamber, in which case we will neglect the velocity increment ($v_0 \approx 0$). In the polytropic case, additional heat is supplied during the expansion. /12

Polytropic:

According to eq.(2.2), the following is generally valid:

$$q = h + \frac{v^2}{2} = h_0\left(\frac{h}{h_0} + \frac{v^2}{2h_0}\right) .$$

With $\frac{h}{h_0} = \frac{T}{T_0} = \left(\frac{p}{p_0}\right)^{\frac{n-1}{n}}$ and eq.(2.5) it follows that

$$\frac{q}{h_0} = \underbrace{\frac{x-1}{x}\cdot\frac{n}{n-1}\left[1 - \frac{x-n}{n(x-1)}\left(\frac{p}{p_0}\right)^{\frac{n-1}{n}}\right]}_{(n > 1)} = \underbrace{\frac{x-1}{x}\cdot\frac{n}{1-n}\left[\frac{x-n}{n(x-1)}\left(\frac{p_0}{p}\right)^{\frac{1-n}{n}} - 1\right]}_{(n < 1)} . \tag{2.8}$$

Isothermal (n = 1):

$$q = h_0 + \frac{v^2}{2} .$$

Substitution of eq.(2.6) will yield

$$\frac{q}{h_0} = 1 + \frac{x-1}{x} \ln \frac{p_0}{p} . \tag{2.9}$$

Adiabatic (n = x):

$$\frac{q}{h_0} = 1 . \tag{2.10}$$

Efficiencies:

Let the efficiency be defined by

$$\eta = \frac{v^2/2}{q}$$

Polytropic:

$$\eta = \frac{1-\left(\frac{p}{p_0}\right)^{\frac{n-1}{n}}}{1-\frac{x-n}{n(x-1)}\left(\frac{p}{p_0}\right)^{\frac{n-1}{n}}} = \frac{\left(\frac{p_0}{p}\right)^{\frac{1-n}{n}}-1}{\frac{x-n}{n(x-1)}\left(\frac{p_0}{p}\right)^{\frac{1-n}{n}}-1} \qquad (2.11)$$

$$(n > 1) \qquad\qquad (n < 1)$$

Isothermal (n = 1): /13

$$\eta = \frac{1}{1+\frac{x}{x-1}\cdot\frac{1}{\ln p_0/p}} \qquad (2.12)$$

Adiabatic (n = x):

$$\eta = 1-\left(\frac{p}{p_0}\right)^{\frac{x-1}{x}} \qquad (2.13)$$

These efficiencies are plotted in Fig.2 as a function of the pressure ratio, for various n at x = 5/3. At $p_0/p \to \infty$, the efficiencies tend toward 1 for the adiabatic, isothermal, and polytropic case at n > 1. For the polytropic case, at n < 1, the following limiting value is obtained:

$$\eta = \frac{n(x-1)}{x-n}.$$

For better illustration, Fig.1 also gives the curves of equal Mach numbers, calculated as follows:

We have

$$M^2 = \left(\frac{v}{c}\right)^2$$

and from

$$c^2 = x\frac{p}{\rho} = (x-1)h$$

it follows that

$$\frac{v^2}{2h_0} = \frac{x-1}{2}M^2\frac{h}{h_0} = \frac{x-1}{2}M^2\left(\frac{p}{p_0}\right)^{\frac{n-1}{n}}$$

Denoting $v^2/2h_0 = \varphi$ and $p_0/p = \pi$, we obtain

$$\pi^{\frac{n-1}{n}} = \frac{x-1}{2}\frac{M^2}{\varphi}$$

$$\frac{n-1}{n} = \frac{\ln\left(\frac{x-1}{2}\frac{M^2}{\varphi}\right)}{\ln \pi}$$

To eliminate n, these expressions are substituted in eq.(2.5) for the polytropic. This yields /14

$$\frac{\varkappa}{\varkappa-1}\varphi = \frac{\ln \pi}{\ln\left(\frac{\varkappa-1}{2}\cdot\frac{M^2}{\varphi}\right)}\cdot\left(1 - \frac{\varphi}{\frac{\varkappa-1}{2}M^2}\right)$$

and, finally, after transformation,

$$\ln \pi = \frac{1}{2}\,\frac{\varkappa M^2}{\frac{\varkappa-1}{2}\cdot\frac{M^2}{\varphi} - 1}\,\ln\left(\frac{\varkappa-1}{2}\,\frac{M^2}{\varphi}\right), \tag{2.14}$$

so that the curves of equal Mach numbers can be plotted in Fig.1. (In this case, it is simpler to calculate π as a function of φ with the parameters M.)

It can be assumed that the actual change of state of an expanding flow with arc heating will be located in the region between the adiabatics and isotherms. A pressure ratio p_0/p of 10^4 to 10^5 seems technically feasible even at the resultant large area ratios between nozzle-end cross section and cross section of the nozzle throat, when considering that plasma engines are relatively small in size and light in weight, compared to the auxiliary power sources.

Using the isotherms as directive, we obtain $v^2/2h_0 \approx 4$ according to Fig.1, at a pressure ratio between 10^4 and 10^5. This means a doubling of the exhaust velocity compared to that obtainable at adiabatic expansion. Figure 2 indicates that the theoretical efficiency decreases in this case from about 98% at adiabatic expansion to about 80% at isothermal expansion.

Above, we gave the maximum obtainable exhaust velocity of electrothermal plasma engines, at adiabatic expansion, as 15,000 m/sec. However, the preceding considerations demonstrate that this velocity can be further increased to about 30,000 m/sec, provided that it is possible to keep the expanding gas in an isothermal state by means of arc heating.

3. Acceleration of Plasma Jets by the Self-Magnetic Field of the Arc /15

In the presence of an arc discharge in an expanding jet, as assumed in the preceding Section, an acceleration effect is produced by the Lorentz forces of the self-magnetic field.

This effect was discovered in 1955 by Maecker (Bibl.3) in investigations on freely burning high-current carbon arcs. Repeatedly, flow phenomena had been observed previous to this, originating from the cathode of an electric arc. Maecker found that an arc, whose column contracts in the vicinity of the cathode, acts like an electromagnetic pump because of the self-magnetic forces, causing the flow to proceed in direction of the divergent arc column.

Figure 3 shows the direction of the Lorentz force $\vec{j} \times \vec{B}$ in the vicinity of the cathode. Together with the magnetic field lines, encircling the arc axis, the divergent $\vec{j}$-field produces $\vec{j} \times \vec{B}$ forces with components in radial and axial direction. The radial components produce the well-known pinch effect and thus a pressure rise in a radial direction, whereas the axial components accelerate the plasma.

The fact, following from these considerations, that not only the cathodic contraction but also any artificial local pinch of the arc column will lead to the formation of plasma jets, was proved experimentally by Maecker.

In a plasma jet, proceeding in a divergent nozzle with superposed arc discharge, the narrowest nozzle cross section will represent such a pinch of the arc column. However, the geometric form of the flow need not be prescribed by a nozzle since, also in rapidly expanding free jets, the required divergence of the discharge cross section takes place.

In Fig.4, a geometric configuration of such a type is plotted. Let r_1 be the radius of a cathode spot or of a nozzle throat. Let the discharge diverge to a radius r_2. If $r_2/r_1 \gg 1$, the entire magnetic thrust S_m, exerted on the plasma in this particular setup, can be calculated. At a low divergence ratio, it is only necessary to know the current density distribution in the cross /16 section F_1. In this case, the current density is assumed as independent of the radius.

Then, the total magnetic thrust, from eq.(1.2) with the relation

$$\int \operatorname{grad} p \, d\tau = \oint p \cdot d\vec{f}$$

is given by

$$\vec{S}_m = \int \vec{j} \times \vec{B} \, d\tau - \oint p_m d\vec{f}, \tag{3.1}$$

where the circular cylinder, shown as a broken line in Fig.4, is selected as integration region and where $d\tau$ denotes one volume element. The second integral is a surface integral of the pressure produced by $\vec{j} \times \vec{B}$ forces.

The first integral can also be transformed into a surface integral. According to eq.(1.4), we first have

$$\vec{j} = \frac{1}{\mu_0} \operatorname{curl} \vec{B}$$

and, with a general vector relation,

$$\vec{j} \times \vec{B} = \frac{1}{\mu_0} [\operatorname{curl} \vec{B} \times \vec{B}] = \frac{1}{\mu_0} (\vec{B} \cdot \operatorname{grad}) \vec{B} - \frac{1}{2\mu_0} \operatorname{grad} B^2. \tag{3.2}$$

Applying Gauss theorem and considering div $\vec{B} = 0$, the volume integral will yield

$$\int \vec{j} \times \vec{B} \, d\tau = \frac{1}{\mu_0} \oint \vec{B} \cdot \vec{B} d\vec{f} - \frac{1}{2\mu_0} \oint B^2 d\vec{f} \tag{3.3}$$

The first surface integral will give zero in this case since, everywhere on the surface, the integration region $\vec{B}$ is perpendicular to $d\vec{f}$. The second integral over $B^2 d\vec{f}$ vanishes on the lateral area of the integration cylinder, since – for symmetry reasons – for each positive $B^2 d\vec{f}$, a negative $B^2 d\vec{f}$ must /17 be present on the opposite side. Similarly, the integral vanishes over the right-hand cylinder cover since, at that point, we have B = 0. On the left-hand cylinder cover, the following is valid for B:

$$0 < r < r_1 \quad : \quad B = \text{[illegible]} \tag{3.4}$$

$$r_1 < r < r_2 \quad : \quad B = \frac{\mu_0}{2} \cdot \frac{I}{\pi r} \; , \tag{3.5}$$

where I denotes the total arc current. Integration will then yield

$$\int \vec{j} \times \vec{B}\, d\tau = -\frac{1}{2\mu_0} \oint B^2 d\vec{f} = \frac{\mu_0 I^2}{4\pi}\left(\frac{1}{4} + \ln \frac{r_2}{r_1}\right). \tag{3.6}$$

Finally, the following expression is obtained for the magnetic pressure p_m produced by the $\vec{j} \times \vec{B}$ forces and occurring only in the cross section F_1, under assumption of constant current density $j = \frac{I}{\pi r_1^2}$ and using eq.(3.4):

$$\frac{dp_m}{dr} = j B = \frac{\mu_0}{2}\left(\frac{I}{\pi r_1^2}\right)^2 \cdot r \tag{3.7}$$

from which, by integration, we obtain

$$p_m = \frac{\mu_0}{4}\left(\frac{I}{\pi r_1^2}\right)^2 (r_1^2 - r^2) . \tag{3.8}$$

Hence,

$$\oint p_m d\vec{f} = 2\pi \int_0^{r_1} p_m\, r\, dr = \frac{\mu_0 I^2}{8\pi} . \tag{3.9}$$

Thus, the total magnetic thrust will become

/18

$$S_m = \frac{\mu_0 I^2}{4\pi}\left(\frac{3}{4} + \ln \frac{r_2}{r_1}\right) = \frac{\mu_0 I^2}{4\pi} \cdot \ln 2.117 \frac{r_2}{r_1} . \tag{3.10}$$

In Fig.5, S_m is plotted as a function of the current intensity for various divergence ratios.

Assuming, for our further discussion, the presence of one-dimensional flow, we have

$$S_m = \dot{m} \cdot \Delta v \; , \tag{3.11}$$

where $\dot{m}$ denotes the weight rate of gas flow, in kg/sec. The expected velocity increments, as a function of the rate of flow, are plotted in Fig.6 at various current intensities, assuming $r_2/r_1 = 10$ as divergence ratio. Prescribing arc current intensities up to 10^4 amp as practically realizable, it will be found that the self-magnetic acceleration effect, at a not excessive gas rate of flow, should yield extremely high velocities up to an order of 10^5 m/sec.

Equation (3.10) can be expressed also in a different form, by setting, in accordance with eq.(1.2),

$$S_m = \int \rho(\vec{v}\cdot\mathrm{grad})\vec{v}\,d\tau = \oint \rho\vec{v}\cdot\vec{v}\,d\vec{f} \tag{3.12}$$

and again applying the surface integral to the model in Fig.4. Assuming one-dimensional flow, this will yield

$$\oint \rho\vec{v}\cdot\vec{v}\,d\vec{f} = \rho_2 v_2^2 F_2 - \rho_1 v_1^2 F_1 = \dot{m}(v_2 - v_1) \tag{3.13}$$

If $v_2 \gg v_1$, eq.(3.10) and $F_2 = \pi r_2^2$ will furnish

$$v_2^2 = \frac{\mu_0}{4\pi}\frac{I^2}{\rho_2 \pi r_2^2}\cdot \ln 2.117\,\frac{r_1}{r_2} \tag{3.14}$$

For illustrating this equation, Fig.7 shows the obtainable velocity for /19
a fully ionized hydrogen plasma jet of $T = 2 \times 10^4$ °K at various pressures, plotted as a function of the current intensity. This diagram indicates that the effect becomes of interest only at high current intensity and low gas densities or gas pressures.

In his experiments, Maecker worked with high-current arcs at atmospheric pressure in the current intensity range up to 300 amp. Accordingly, the calculated maximum velocity in the arc axis was only 300 m/sec, a value experimentally confirmed later by Wienecke (Bibl.4). Maecker was also able to measure the increased gas pressure and the recoil on the cathode. These values are low at normal pressure and moderate current intensities: At 300 amp current intensity, the positive magnetic pressure in front of the cathode will be 100 mm water column and the recoil on the cathode will be approximately 1 pond*. However, even with these low forces, Maecker was able to drive an "arc carrousel" (Bibl.3).

---

* pond = weight of the mass unit of one gram at the locus of normal gravitational acceleration (980.665 cm/sec^2).

Despite the fact that the magnetic forces, at moderate current intensities and at atmospheric pressure, are extremely low, the jet formation has a noticeable influence on the total energy transport within the arc. For this reason, one of the authors in an earlier paper (Bibl.5) mentioned that, in designing arc chambers for the production of plasma jets, this jet-forming effect naturally should be utilized, specifically since this magnetically driven flow increases rapidly with increasing current intensity and since the gas to be heated should be supplied to all combustion chambers at the cathode end.

It should be mentioned here that reports from the USA (Bibl.6) indicate that the Giannini Corporation, Avco Corporation, and Electro-Optical Systems have been able to produce velocities up to 10^5 m/sec at a thrust of about 200 gm with a so-called "hybrid thruster" at high current intensities and low gas pressures. These data can be used for calculating a weight rate of gas flow of 2×10^{-5} kg/sec. Figure 6 shows that a velocity of 10^5 m/sec at this rate of flow can be obtained at a current intensity of 2000 amp. Therefore, it can be assumed that these novel plasma jet generators operate with the above-described self-magnetic acceleration.

4. Experimental Investigations /20

In the attempt to realize arc heating as well as self-magnetic acceleration in an expanding supersonic plasma flow a prime assumption is that a high-current arc will be stable in such a flow, under negative pressure conditions.

In treating this problem, both authors (Bibl.7) came independently to the same experimental setup, as sketched in Fig.8.

The left-hand side shows a conventional plasma burner with convergent nozzle section. The arc burns under normal pressure between the cathodic tungsten point and the nozzle wall which acts as the anode (anode I). At a sufficiently narrow nozzle end diameter, sonic velocity is reached at the narrowest point. This arrangement is placed in a vacuum tank which can be pumped continuously to a pressure of 1 torr. Because of the great pressure difference, the plasma jet expands rapidly under formation of a bell-shaped expansion fan to supersonic velocity (Fig.9).

In this manner, two important requirements for the production of self-magnetic acceleration, namely, low gas density and large divergence ratio r_2/r_1 are already prescribed by the flow. After this, the anode II, installed at the point at which the expanding jet reaches its maximum diameter, is connected and the anode I is disconnected. The high-current arc will now operate within the high-pressure region inside the chamber as well as within the expanding flow in the low-pressure region. Figure 10 shows this state, with the anode II connected. Because of the arc heating, the jet divergence is greater here than in Fig.9.

In these experiments, performed in the DVL* Institute for Plasma Dynamics, the current intensity in stationary operation with argon was 230 amp, at an arc potential of 45 v. The ambient pressure in the vacuum chamber was set to 1 torr.

The setup, used in the Electrophysics Department of the Polytechnic Institute in Munich differs merely by the fact that a ring anode of graphite was used instead of the spiral anode II of copper tubing. In addition, the insulating /21 plate of boron nitride at the end of the plasma burner, shown in Fig.8, was replaced by an electrically insulated and separately cooled metal plate. In Fig.11, the ambient pressure is 5 torr. The current intensity, again for

---

* DVL = German Aeronautics and Space Experiment Station.

operation with argon, is 120 amp with the corresponding arc potential being 70 v. A smaller divergence of the expansion fan, at equal electric data is obtained (as shown in Fig.12) at an ambient pressure of 20 torr. In this case, a portion of the jet boundary strikes the graphite ring at high velocity and is vertically deflected, so that a "plasma slab" is formed.

In these experiments, it was primarily a question to demonstrate that an arc discharge is stable in an expanding supersonic flow and that the requirements necessary for effectiveness of the self-magnetic acceleration, such as low gas density and large divergence ratio, can be prescribed by the flow.

The experiments are being continued with helium and hydrogen at higher current intensities.

5. Summary and Future Aspects

With respect to classical gas dynamics, two electrodynamic terms occur in the fundamental equations of plasma dynamics, namely, the Lorentz force $\vec{j} \times \vec{B}$ in the momentum equation and the Joule heat $\vec{j} \cdot \vec{E}$ in the energy equation, which both are of importance for the problems of plasma acceleration. An investigation is made as to the manner in which both effects, in a stationary plasma flow with superposed arc discharge, can contribute to the production of high plasma velocities. Although these effects become superimposed in practical designs, their influence is discussed separately for greater clarity. In both cases, the possibility is assumed that an electric arc is able to exist at all in an expanding supersonic flow at negative pressure.

In considering the possibility of liberating Joule heat $\vec{j} \cdot \vec{E}$ at any state of flow, the problem of reheating in an arbitrary nozzle flow is involved. For a simplified thermodynamic theory, polytropic changes of state are assumed in which the adiabatic and the isothermal expansion occur as special cases and which, for practical considerations, must be considered to be limiting cases. /22

The limiting case of adiabatic expansion has been approximately realized in all existing electrothermal plasma drives, in which gases are heated in a combustion chamber by an electric arc and then are expanded in a nozzle without further supply of heat. The maximum velocity, obtainable with this method, is defined by the enthalpy of the gas in the combustion chamber. However, since this enthalpy cannot be increased arbitrarily because of problems of cooling technique, the attainable velocity is limited despite the fact that it is far above the gas velocities obtainable with chemical reactions. For example, for the mentioned electrothermal plasma burners, this critical velocity is given as about 15,000 m/sec on operation with hydrogen.

Higher velocities, at equal combustion chamber enthalpy, should be obtainable by reheating the plasma during the expansion. This can be realized by extending the arc discharge through the entire expansion nozzle. If, in this case, an isothermal expansion is considered the upper limiting case obtainable in practice, thermodynamic calculations (Fig.1) show that the velocity increases arbitrarily with increasing pressure ratio between combustion chamber pressure and nozzle end pressure. For technical reasons (nozzle cross sections, etc.), a pressure ratio of 10^5 cannot be exceeded by much, so that - in the extreme case - a velocity increment by a factor of 2 can be expected (Fig.1).

The existence of an electric arc in a divergent stream filament is accompanied by an acceleration effect produced by the $\vec{j} \times \vec{B}$ forces of the self-magnetic field. This effect was discovered in 1955 by Maecker on a free-burning high-current arc. An analysis shows that the obtainable velocity, according to eq.(3.10), increases at constant rate of flow with the square of the current intensity. Considering an arc current intensity of 10^4 amp, at a completely conventional gas rate of flow of 10^{-4} kg/sec in plasma burners, as technically realizable, velocities up to 10^5 m/sec should occur according to Fig.6. Such velocities have been considered as characteristic for ion engines and pulsed electromagnetic propulsion systems.

The experimental investigations primarily had the purpose of checking /23 whether an arc discharge, in an expanding supersonic flow at negative pressure, is able to exist and remain stable. This question was answered in the positive sense on the basis of experimental setups independently developed at the DVL Institute for Plasma Dynamics and at the Electrophysics Department of the Polytechnic Institute, Munich. The experiments, made until now with argon at moderate current intensities are being continued with helium and hydrogen at high current intensities.

In a further experimental unit, the expansion is to be produced with a superposed arc in an expansion nozzle which, as shown in Fig.13, is composed in accordance with Maecker's "cascade" principle (Bibl.8) of individual insulated and cooled copper plates, using the end plate as anode. This "cascade" principle prevents a migration of the arc current through the nozzle walls to the anode.

In addition, an attempt will be made to increase the magnetic acceleration by superposition of an external field. Our discussions referred only to the self-magnetic field of the arc, whose size and direction is given by the Maxwell equation (1.4) from the current-density distribution in the arc.

An external field, which is independent of the arc discharge, can be made much stronger than the self-magnetic field of the arc. The only difficulty lies in the fact that only azimuthal field components, together with the current

density component of the arc, lead to an acceleration in axial direction. The arrangement of an axial magnetic field will result only in a rotation of the entire arc plasma. In accordance with the self-magnetic field of the arc, a closed purely azimuthal field can be produced only in the direct vicinity of an axisymmetric conductor. However, the presence of such a conductor within the hot plasma jet is inconceivable for cooling-technology reasons. Nevertheless, at least local azimuthal field components can be produced by winding helical conductor couples around the divergent discharge space (Fig.14), a method used in the "stellarator" for stabilization processes. Whereas, in the stellarator machine, adjacent turns carry currents of opposite directions, all currents /24
in the above device must be rectified so as to obtain a uniform sense of direction for all local azimuthal components. Since, when using helical turns, also axial field components will occur, a rotation of the accelerated plasma flow cannot be avoided.

In summation, we can state the following: In space problems, the required exhaust velocities of the power plants, depending on the optimizing conditions, will be in the range of 10^4 to 10^5 m/sec and beyond. In the region up to 3×10^4 m/sec, electrothermal engines with arc heating and reheating during the expansion presumably will be found useful. Beyond this, the magnetic acceleration effect will predominate, in which case - provided that current intensities of 10^4 amp per propulsive unit are considered as the technically attainable limit - a mass rate of flow of only $\dot{m} < 10^{-4}$ kg/sec can be expected.

Finally, it should be mentioned that stationary plasma jets with velocities of the order of 10^5 m/sec are of importance not only for plasma drives but also generally for plasma physics, since these velocities correspond to extremely high stagnation temperatures (Fig.15)*. (for footnote see following page).

6. Appendix

/25

a) List of Symbols

v = velocity of flow

ρ = density

p = pressure

h = enthalpy

w = heat flux density

j = electric current density

B = magnetic induction

E = electric field strength

$\mu_0 = 4\pi \cdot 10^{-7} \left[\frac{Vs}{Am}\right]$ = induction constant

$\vec{j} \times \vec{B}$ = Lorentz force

$\vec{j} \cdot \vec{E}$ = Joule heat

q = heat supplied per mass unit

$k = 1.38 \times 10^{-23} \left(\frac{\text{w-sec}}{^{\circ}K}\right)$ = Boltzmann constant

T = temperature

m = mass of the atom or molecule

x = ratio of specific heats

n = polytropic exponent

μ = efficiency /26

M = Mach number

c = velocity of sound

$\pi = p_0/p$ = pressure ratio

---

* After completion of the manuscript, a scientific paper was published in the 1964 August issue of the AIAA Journal, giving experimental data obtained at the Giannini Corporation (Bibl.9).

$\varphi = v^2/2h_0$ = abbreviation

S_m = magnetically produced thrust

p_m = magnetically produced pressure

r = radius

r_2/r_1 = divergence ratio

I = current intensity

$\dot{m}$ = gas rate of flow

BIBLIOGRAPHY /27

1. Ackeret, J.: A System of Rocket Propulsion Using Reactors and Gas Turbines. Proc. IX Intern. Astronautical Congr., Amsterdam, 1958, Vol.I, pp.277-281, Springer-Vienna, 1959.
2. Winterberg, F.: Attainment of Exhaust Velocities up to 20,000 m/sec by Isothermal Expansion in Nuclear Rockets (Die Erreichung von Ausströmgeschwindigkeiten bis 20 000 m/s durch isotherme Expansion in Kernraketen). Proc. IX Intern. Astronautical Congr., Amsterdam, 1958, Vol.I, pp.181-199, Springer-Vienna, 1959.
3. Maecker, H.: Plasma Flows in Electric Arcs, due to Self-Magnetic Compression (Plasmaströmungen in Lichtbögen infolge eigenmagnetischer Kompression). Z. Physik, Vol.141, pp.198-216, 1955.
4. Wienecke, R.: The Velocity Field of the High-Current Arc Column (Über das Geschwindigkeitsfeld der Hochstromkohlebogensäule). Z. Physik, Vol.143, pp.128-140, 1955.
5. Peters, Th.: Production of Plasma Jets of High Temperatures and Velocities (Erzeugung von Plasmastrahlen hoher Temperaturen und Geschwindigkeiten). Astronaut. Acta, Vol.7, pp.150-170, 1961.

6. Yaffee, M.L.: Three Firms Developing Hybrid Thruster. Aviation Week and Space Technology, p.65, March 23, 1964.

7. Peters, Th.: Plasma Acceleration in an Expanding Supersonic Flow (Plasmabeschleunigung in expandierender Überschallströmung). Z. Naturforsch., in Press.

8. Maecker, H.: A Cylindrical Arc for High Performance (Ein zylindrischer Bogen für hohe Leistungen). Z. Naturforsch., Vol.11a, pp.457-459, 1956.

9. Ducati, A.C., Giannini, G.M., and Muehlenberger, E.: Experimental Results in High-Specific Impulse Thermionic Acceleration. AIAA-J., Vol.2, pp.1452-1454, 1964.

List of Illustrations

Fig.1: Ratio $v^2/2h_o$ as a Function of the Pressure Ratio p_o/p (Combustion-Chamber Pressure to Nozzle End Pressure) at Polytropic Expansion Plotted for Various Polytropic Exponents n ($x = 5/3$). Here, h_o denotes the enthalpy in the combustion chamber. The curves of constant Mach number are shown as broken lines and represent curves of constant efficiency (see Fig.2).

Fig.2: Efficiencies μ at Polytropic Expansion, as a Function of the Pressure Ratio p_o/p for Various Polytropic Exponents n ($x = 5/3$). Generally, the relation $\mu = \dfrac{1}{1 + \dfrac{2}{(x-1)M^2}}$ is valid and for $x = 5/3$, we have $\mu = \dfrac{1}{1 + 3/M^2}$. Therefore, a Mach number M can be coordinated with each μ (see right-hand scale).

Fig.3: Direction of the Lorentz force $\vec{j} \times \vec{B}$ in an Arc Column, Pinched by the Cathode Spot. /28

Fig.4: Geometric Configuration of an Arc Discharge, Diverging from the Cross Section F_1 to F_2. Divergence ratio of the radii r_2/r_1. The broken-line cylinder is used for calculating the total magnetically produced thrust S_m.

Fig.5: Magnetically Produced Thrust S_m in Newtons, as a Function of the Arc Current I for Various Divergence Ratios r_2/r_1.

Fig.6: Velocity Increment Δv, Based on Self-Magnetic Acceleration, as a Function of the Gas Rate of Flow $\dot{m}$ at Various Current Intensities for $r_2/r_1 = 10$.

Fig.7: Example for the Velocity Obtainable by Self-Magnetic Acceleration of a Fully-Ionized Hydrogen Plasma, Discharged at $T = 2 \times 10^4$ °K, as a Function of the Arc Current Intensity for Various End Pressures p or Gas Densities ρ. The radius of the end face F_2 (jet radius) is assumed as $r_2 = 0.05$ m.

Fig.8: Arrangement for Producing a Rapidly Expanding Plasma Flow, with Plasma Burner and Auxiliary Anode in the Negative Pressure Region.

Fig.9: Divergence of the Plasma Jet in the Negative Pressure Region. Heating between cathode and anode I (see Fig.8). (Photograph: DVL Institute for Plasma Dynamics).

Fig.10: Plasma Jet with Heating between Cathode and Anode II. Anode I is disconnected (see Fig.8). The electric arc burns here in the high-pressure portion of the plasma burner as well as in the expanding supersonic flow in the negative pressure region. I = 230 amp, 45 v, p = 1 torr, argon, $r_1 = 3$ mm, $r_2 > 35$ mm. (Photograph: DVL Institute for Plasma Dynamics).

Fig.11: Photograph of the Setup with Graphite Ring as Anode II, from the /29

Electrophysics Department of the Polytechnic Institute, Munich. I = 120 amp, 70 v, p = 5 torr, argon.

Fig.12: Photograph from the Electrophysics Department of the Polytechnic Institute, Munich. I = 120 amp, 70 v, p = 20 torr, argon. A portion of the boundary flow is deflected by the graphite ring and forms a "plasma slab".

Fig.13: Design of an Expansion Nozzle according to Maecker's "Cascade" Principle. The individual disks are separately cooled and electrically insulated, so that the arc current cannot migrate within the nozzle wall to the anode. The end face is formed by the anode.

Fig.14: Application of an External Magnetic Field for Increasing the Magnetic Acceleration. Helically wound conductors surround the expansion fan in which the electric arc is operating. The left-hand cylindrical portion contains no field lines. At the right, the magnetic field gradually passes into an axisymmetric guide field.

Fig.15: Stagnation Temperatures of a Fully Ionized Hydrogen Plasma, as a Function of the Flow Velocity. ΔT = temperature difference between stagnation temperature and temperature in the flow. T_0 = stagnation temperature and $T = 2 \times 10^4$ °K in the flow (see example in Fig.7).

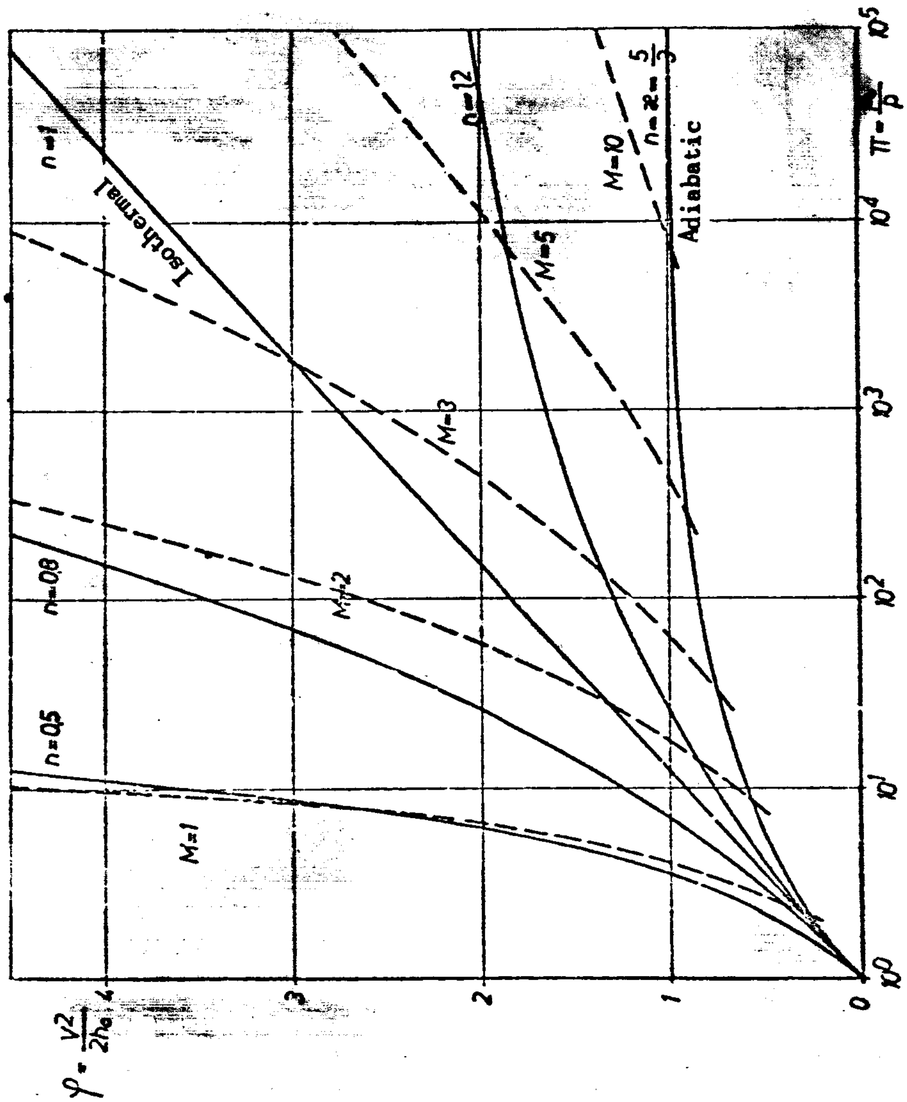
Isothermal
Adiabatic
n=1
n=0.8
n=0.5
n=12
M=1
M=2
M=3
M=5
M=10
0
1
2
3
4
10^0
10^1
10^2
10^3
10^4
10^5

Fig.1

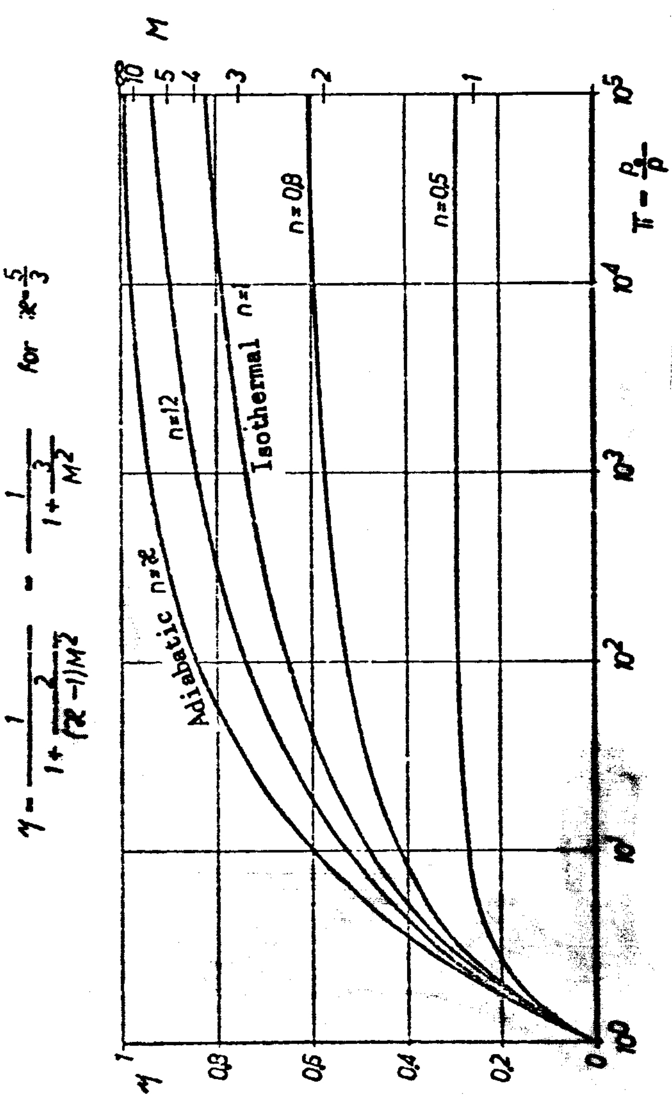
η = 1 / (1 + 2/((κ − 1)M²)) = 1 / (1 + 3/M²)   for κ = 5/3
Adiabatic n=κ
n=1.2
Isothermal n=1
n=0.8
n=0.5
η
1
0.8
0.6
0.4
0.2
0
10^0
10^1
10^2
10^3
10^4
10^5
π = p_0/p
M
∞
10
5
4
3
2
1

Fig.2

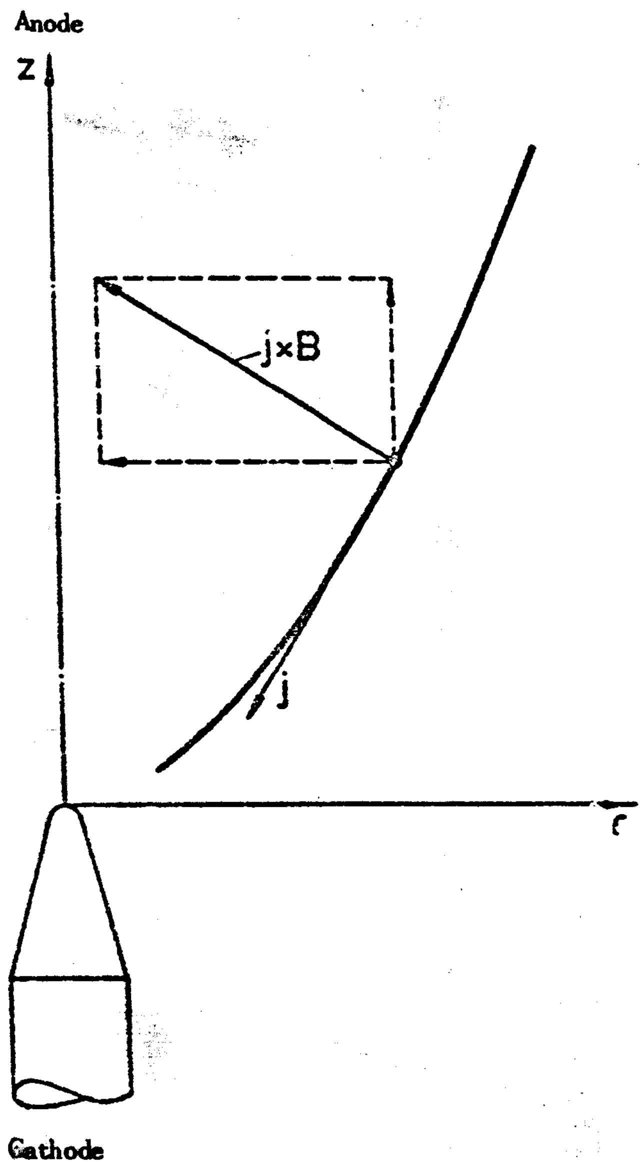

Fig.3

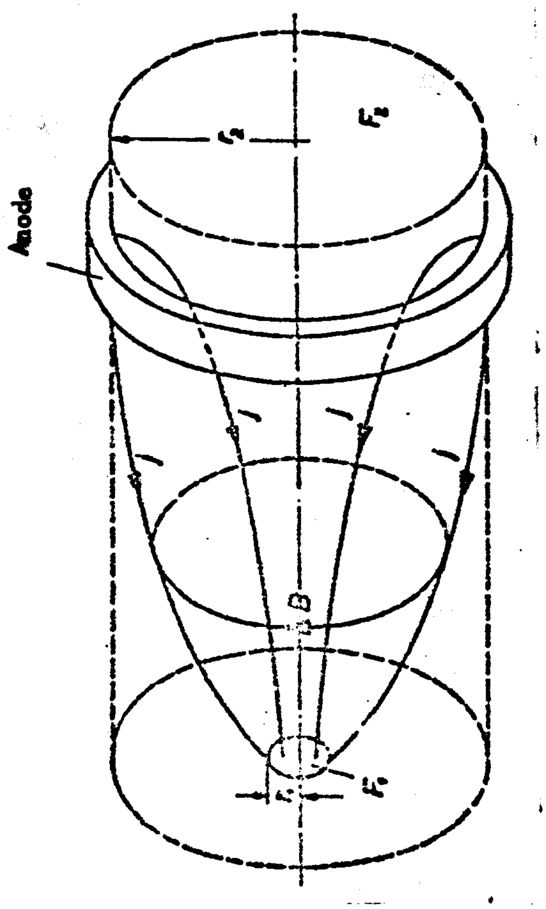

Fig.4

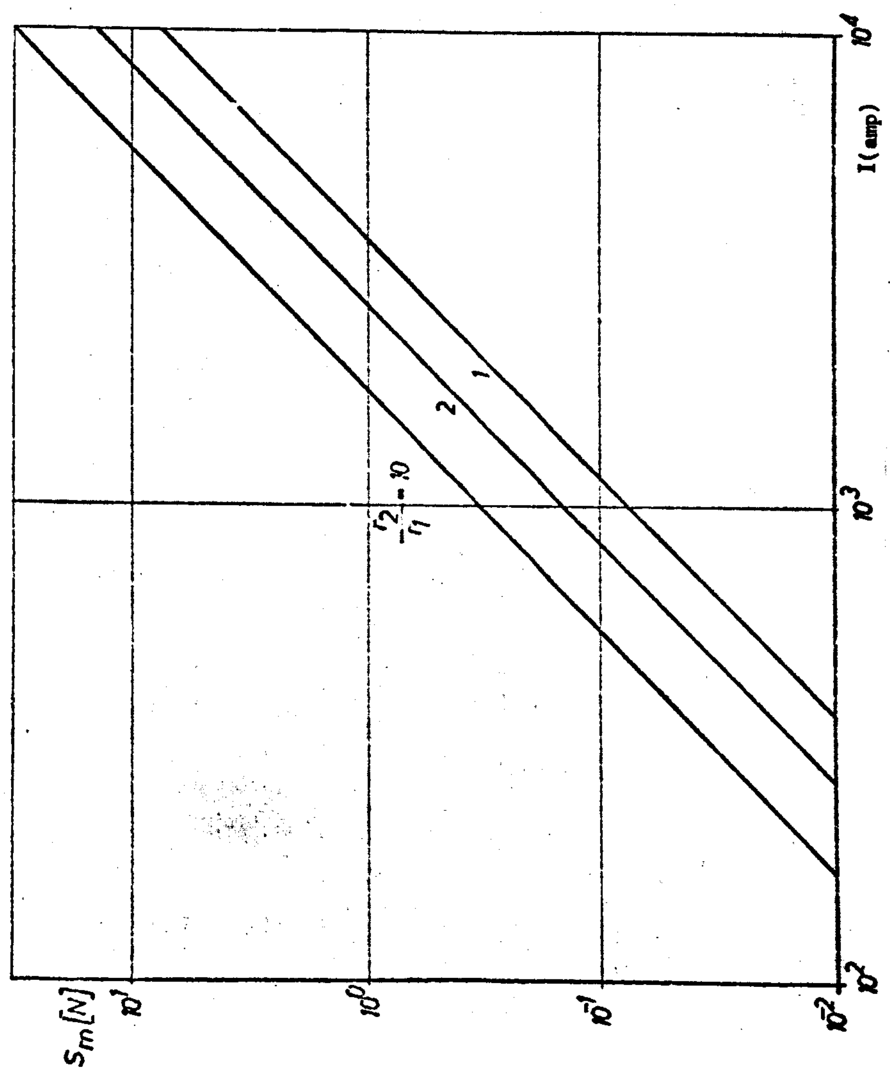

Fig.5

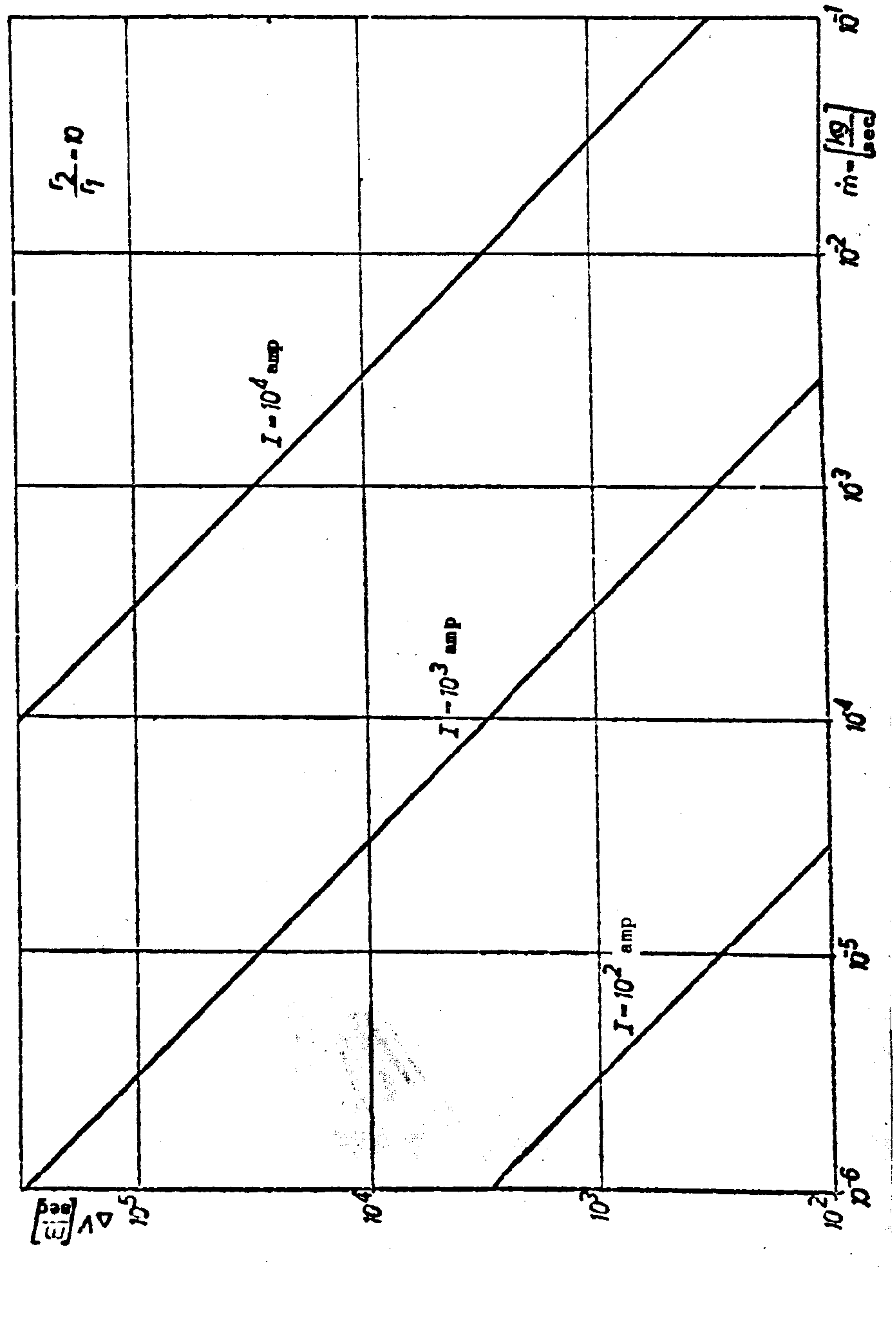
r2/r1 = 10
ṁ = [kg/sec]
I = 10^4 amp
I = 10^3 amp
I = 10^2 amp
ΔV [m/sec]
10^5
10^4
10^3
10^2
10^-1
10^-2
10^-3
10^-4
10^-5
10^-6

Fig.6

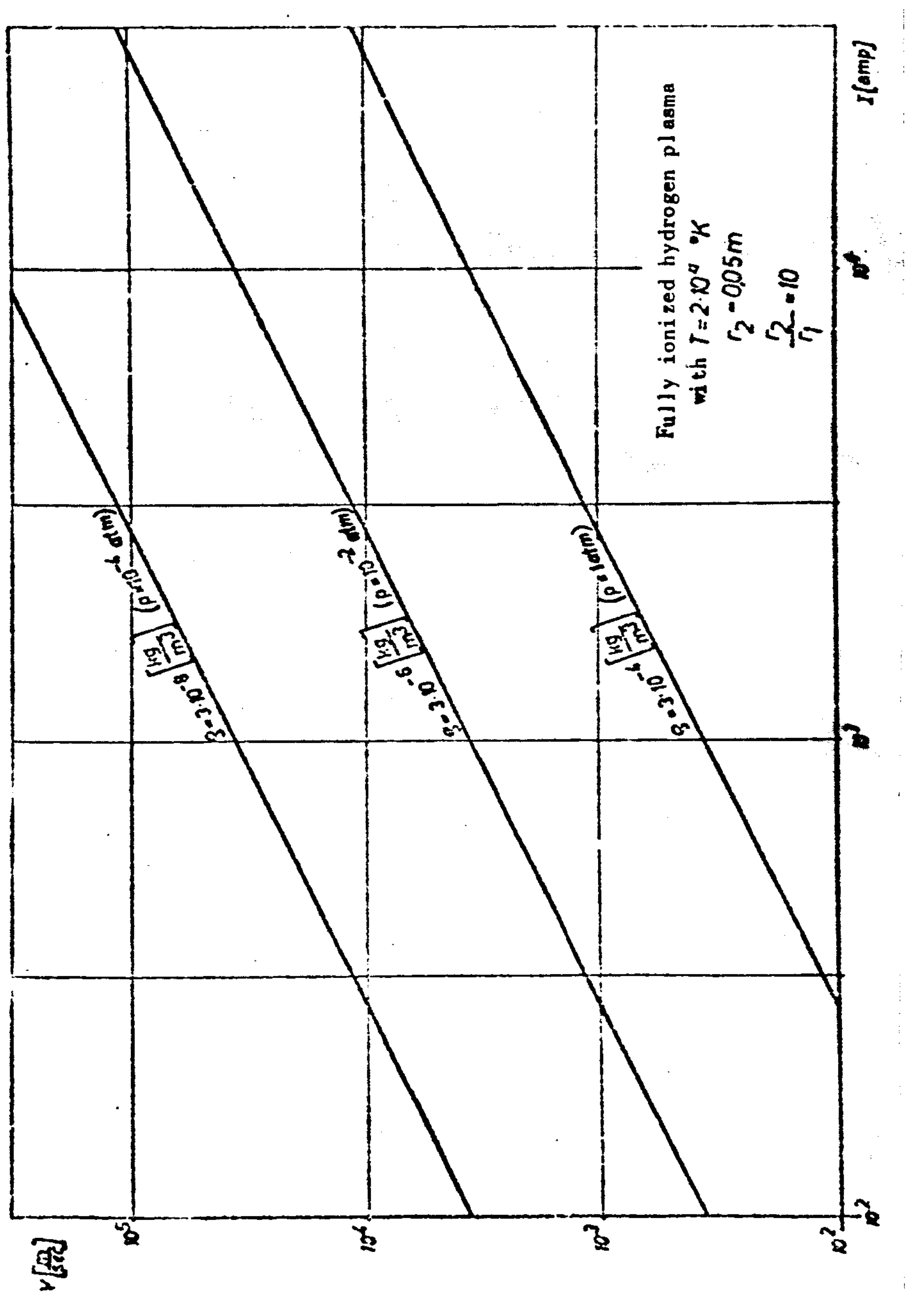

v [m/sec]
10^5
10^4
10^3
10^2
10^2
10^3
10^4
I [amp]
ρ = 3·10^-8 [kg/m3] (p = 10^-4 atm)
ρ = 3·10^-6 [kg/m3] (p = 10^-2 atm)
ρ = 3·10^-4 [kg/m3] (p = 1 atm)
Fully ionized hydrogen plasma
with T = 2·10^4 °K
r2 = 0,05m
r2/r1 = 10

Fig. 7

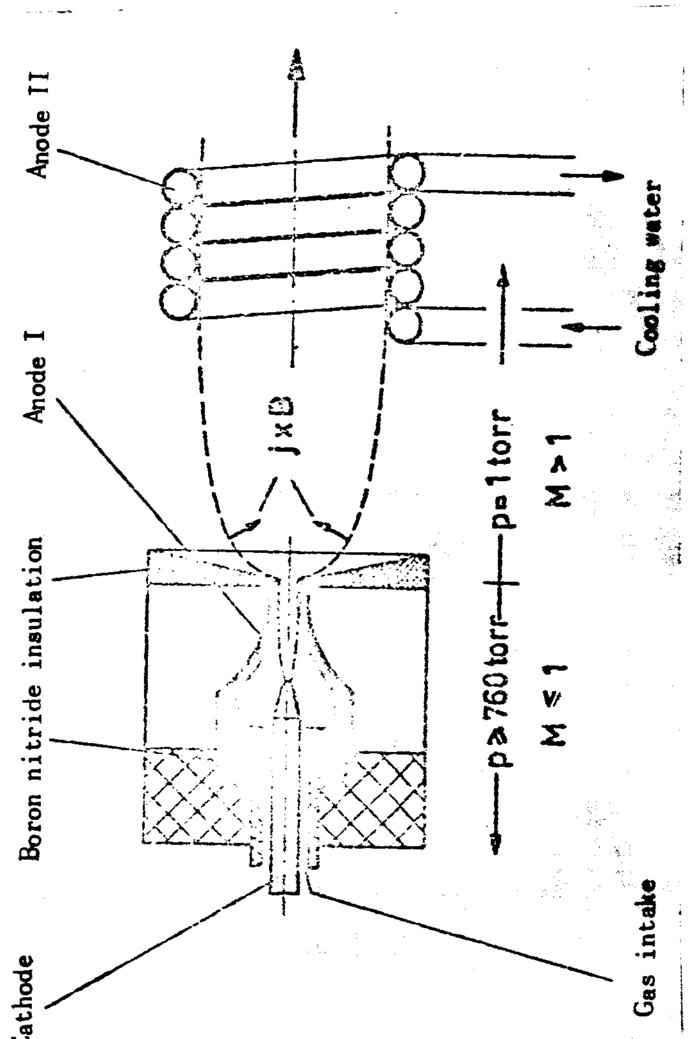

Cathode
Boron nitride insulation
Anode I
Anode II
j x B
Cooling water
Gas intake
p ≥ 760 torr
p = 1 torr
M ≤ 1
M > 1

Fig.8

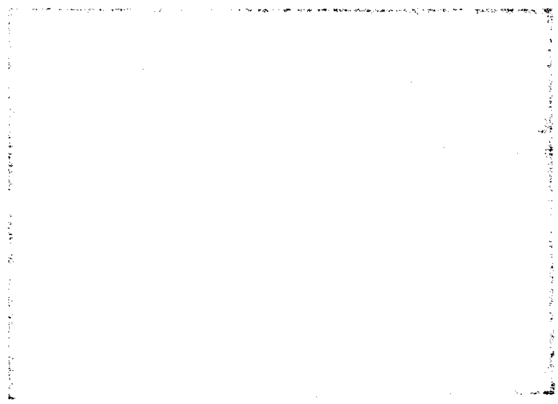

Fig.9

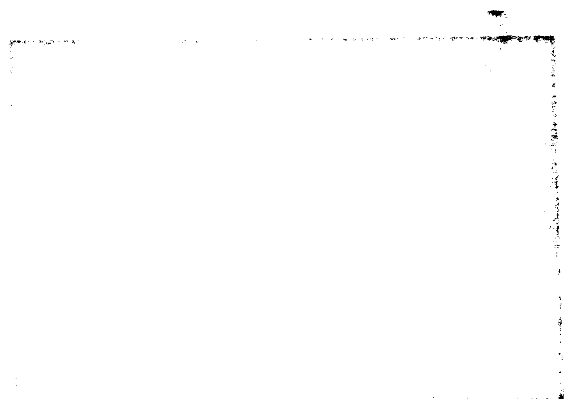

Fig.10

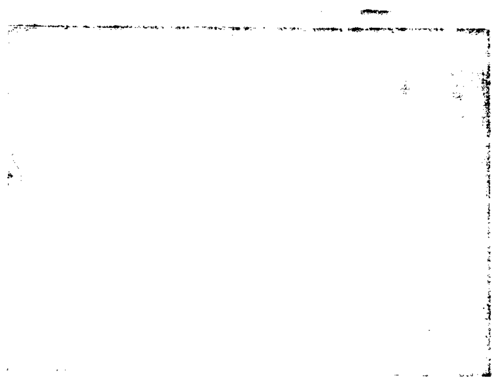

Fig.11

Fig.12

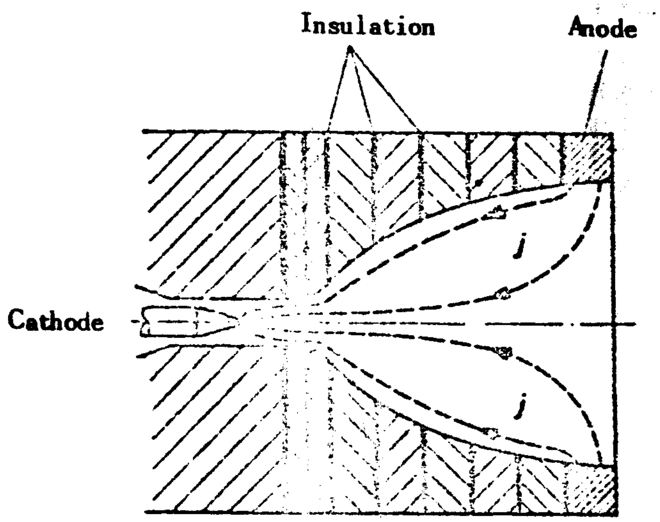

Fig.13

Fig.14

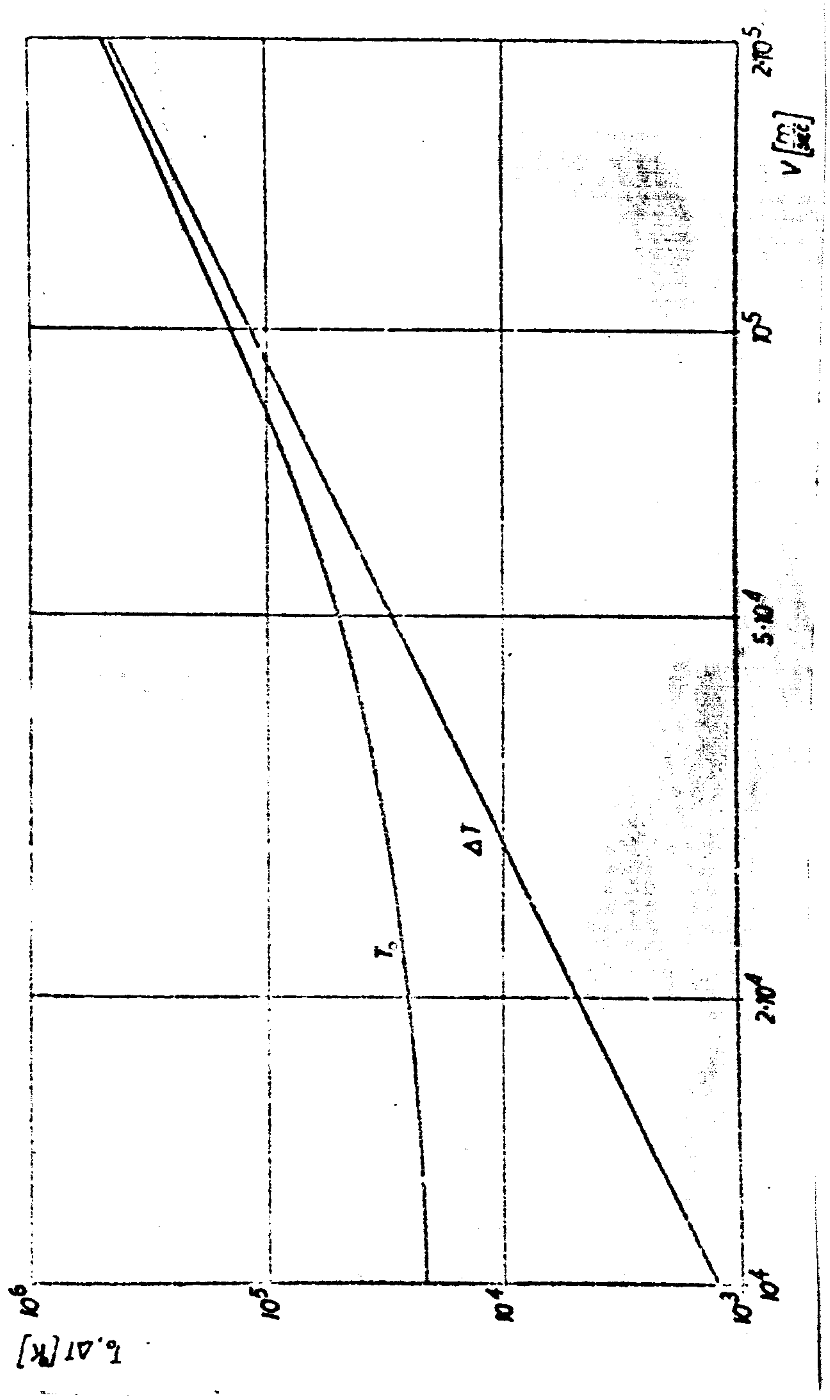

Fig.15

Translated for the National Aeronautics and Space Administration by the O.W.Leibiger Research Laboratories, Inc.